Available online at www.sciencedirect.com
SCIENCE DIRECT®
C. R. Chimie 7 (2004) 1165–1172
COMPTES RENDUS CHIMIE
http://france.elsevier.com/direct/CRAS2C/

Full paper / Mémoire

Titanate-based ceramics for separated long-lived radionuclides

Catherine Fillet *, Thierry Advocat, Florence Bart, Gilles Leturcq, Hélène Rabiller

Commissariat à l'énergie atomique (CEA Marcoule), DEN/DIEC, BP 17171, 30207 Bagnols-sur-Cèze cedex, France

Received 15 September 2003; accepted after revision 5 February 2004

Available online 17 September 2004

Abstract

Studies have been conducted in France to minimize the potential long-term impact of nuclear waste by enhanced chemical separation of the minor actinides (Np, Am, Cm) and some long-lived fission products (I, Cs, Tc). Two options may be considered following this work: (*i*) the initial reference option is transmutation by neutron bombardment in nuclear facilities, (*ii*) the second option would be to incorporate the separated elements into an inorganic matrix ensuring long-term stability. In the case of specific conditioning, zirconolite and hollandite are the potential host phases for the minor actinides and caesium, respectively. Both of these matrices have shown strong potential: (*i*) for incorporating the respective radioelement in the crystalline structure, (*ii*) for fabricating the ceramic by natural sintering in air, (*iii*) for chemical durability with a very low initial alteration rate (about 10^{-2} g m^{-2} d^{-1} at 100 °C), then very rapidly reach alteration rates more than four orders of magnitude lower. In the case of zirconolite ceramics, the high chemical durability is conserved even after amorphization of the crystalline structure by external irradiation with heavy ions or by self-irradiation in natural zirconolites 550 million years old. ***To cite this article: C. Fillet et al., C. R. Chimie 7 (2004).***

Résumé

Pour réduire l'impact potentiel à long terme des déchets nucléaires, des études sont conduites en France sur la séparation chimique poussée des actinides mineurs (Np, Am, Cm) et de certains produits de fission à vie longue (I, Cs, Tc). À l'issue de cette étape, deux options sont envisageables : (*i*) la transmutation par bombardement neutronique dans des systèmes nucléaires est la première option de référence, (*ii*) la seconde option consisterait à incorporer les éléments séparés des autres déchets nucléaires dans une matrice minérale stable à long terme. Dans le cadre d'un conditionnement spécifique, la zirconolite et la hollandite sont des phases hôtes potentielles respectivement pour les actinides mineurs et le césium. Ces deux matrices ont montré une potentialité élevée (*i*) d'incorporation du radioélément considéré dans la structure cristalline, (*ii*) d'élaboration de la céramique par des procédés de frittage naturel sous air, (*iii*) de durabilité chimique, avec une vitesse initiale d'altération très faible (de l'ordre de 10^{-2} g m^{-2} j^{-1} à 100 °C), puis très rapidement des diminutions des vitesses d'altération de plus de quatre ordres de grandeur. Pour la céramique zirconolite, cette propriété de durabilité chimique élevée reste conservée, même après amorphisa-

* Corresponding author.
E-mail address: catherine.fillet@cea.fr (C. Fillet).

1631-0748/$ - see front matter © 2004 Académie des sciences. Published by Elsevier SAS. All rights reserved.
doi:10.1016/j.crci.2004.02.018

tion de la structure cristalline par irradiation externe aux ions lourds ou par auto-irradiation sur des zirconolite naturelles âgées de 550 millions d'années. ***Pour citer cet article : C. Fillet et al., C. R. Chimie 7 (2004).***

Keywords: Conditioning; Zirconolite; Hollandite; Chemical durability

Mots clés : Conditionnement ; Zirconolite ; Hollandite ; Durabilité chimique

1. Introduction

Studies have been conducted in France to minimize the potential long-term impact of nuclear waste by enhanced chemical separation of the minor actinides (Np, Am, Cm) and some long-lived fission products (I, Cs, Tc) for transmutation or for specific conditioning.

The specific conditioning route raises several issues that must be addressed:

- suitability of the matrix for incorporation of appreciable quantities of the desired radionuclide at atomic scale;
- long-term resistance to the effects of self-irradiation;
- resistance to aqueous corrosion.

Titanate-based ceramics (Synroc) developed by ANSTO (Australia) to condition fission product solutions have demonstrated substantial containment capacity [1]. Zirconolite and hollandite (main phases in Synroc ceramic) are thus being considered as potential host phases for conditioning minor actinides and caesium, respectively.

2. Zirconolite

Zirconolite $CaZr_xTi_{2-x}O_7$ ($0.8 < x < 1.37$) has a lamellar monoclinic structure with space group $C_{2/c}$ (Fig. 1). Layers comprising CaO_8 and ZrO_7 polyhedra are stacked with layers consisting of titanium TiO_6 and TiO_5 polyhedra; stacking occurs parallel with the crystal plane [001]. Three loading schemes for the actinides (An) or their surrogates (rare earth elements) have been demonstrated experimentally, showing that these elements can be incorporated into the Ca or Zr sites of the structure with Al as charge compensator [2–5]:

- $Ca_{1-x}An_x^{3+}ZrTi_{2-x}Al_xO_7$ for the trivalent elements,
- $Ca_{1-x}An_x^{4+}ZrTi_{2-2x}Al_{2x}O_7$ for the tetravalent elements,
- $CaZr_{1-x}An_x^{4+}Ti_2O_7$ for the tetravalent elements.

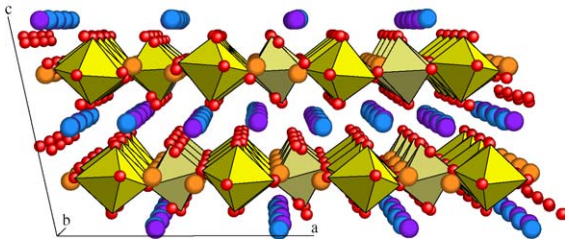

Fig. 1. Crystalline structure of zirconolite 2M $CaZrTi_2O_7$ (88 atoms per cell), where $a = 12.45$ Å, $b = 7.11$ Å, $c = 11.32$ Å and $\beta = 102.37°$. The layers formed by polyhedra of Ca (blue) and Zr (violet) ions alternate with layers of 6-coordinated Ti ions (yellow octahedra) and 5-coordinated Ti with 50% occupancy (orange). O^{2-} anions are shown in red (spheres of arbitrary size).

These loading schemes ensure chemical flexibility within the zirconolite.

2.1. Synthesis and characterization of Nd-doped zirconolite

Nd-doped zirconolite $Ca_{0.8}Nd_{0.2}ZrTi_{1.8}Al_{0.2}O_7$ (Nd used as surrogate for the trivalent actinides 10% in weight) is synthesized through the following steps [6]. First, an amorphous homogeneous powder precursor is obtained by hydrolysis of a mixture of Al, Zr, and Ti alkoxides by a nitric acid solution of Ca and Nd. After hydrolysis, the resulting powder is oven-dried at 120 °C, then calcined for 2 h at 750 °C and ground. The powder is then pressed at 40 MPa to obtain cylindrical compacts that are sintered in air at 1400 °C for between 4 and 96 h. To prevent the formation of perovskite $CaTiO_3$ (a secondary phase capable of containing actinides with relatively lower chemical durability than zirconolite), which frequently appears while synthesizing zirconolite [7], 1.5 wt% excess TiO_2 and ZrO_2 are added to the initial composition. Zirconolite is the predominant phase (99.5% measured by image analysis) (Fig. 2); the minor phase $ZrTiO_4$ (0.5%) is not detectable by XRD (Fig. 3).

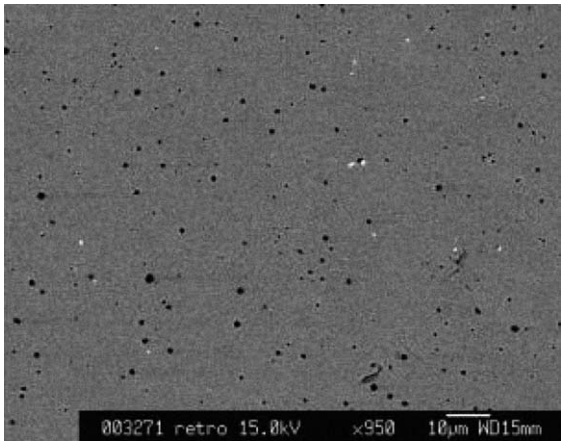

Fig. 2. Backscattered electron image of zirconolite ceramic $Ca_{0.8}Nd_{0.2}ZrTi_{1.8}Al_{0.2}O_7$ (× 950). The small white dots are $ZrTiO_4$, the black one are porosity.

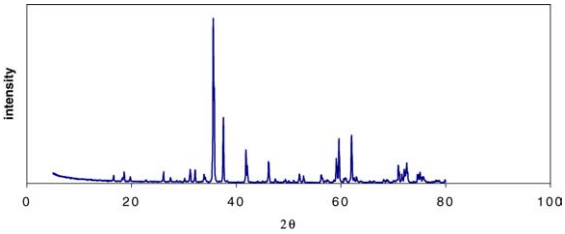

Fig. 3. X-ray diffractogram of zirconolite ceramic $Ca_{0.8}Nd_{0.2}ZrTi_{1.8}Al_{0.2}O_7$(Co Kα radiation): all peaks are indexed 2M zirconolite.

2.2. Chemical durability

Since these conditioning matrices are intended for disposal in a geological environment, they may come into contact with groundwater; assessing their chemical durability properties is thus a major issue.

The chemical durability of the matrix is assessed (*i*) through tests in pure water on inactive ceramics containing rare-earth elements to describe the alteration mechanisms, (*ii*) on ceramics irradiated by external irradiation with charged particles or by self-irradiation (notably for matrices doped with short-lived actinides). During this phase, natural analogues also provide a significant contribution.

2.2.1. Chemical durability of zirconolite ceramic

The initial alteration rates r_0 in initially pure water were determined between 50 and 200 °C using the following conditions: low *SA/V* ratios (surface area to volume of the leachate), high renewal rate of solution, short duration tests (few days). The initial alteration rates r_0 is calculated by assaying calcium (an alteration tracer) in solution [8]. The activation energy E_a of the hydrolysis reaction is about 15 to 30 kJ mol^{-1} (Fig. 4). At 100 °C, the initial alteration rate of zirconolite is about 10^{-2} g m^{-2} d^{-1}, at 200 °C it is about 10^{-1} g m^{-2} d^{-1}; this result shows a moderate increase of the dissolution rate with temperature. Moreover, the initial dissolution step is transient (lasting a few hours to a maximum of 1 day); the rate then diminishes very rapidly toward r_t (i.e. the rate under 'saturation' conditions).

The variation of the alteration kinetics over time was assessed by means of experiments with powder or monoliths at various *SA/V* ratios (0.1 to 287 cm^{-1}) over periods ranging from several months to several years at temperatures between 50 and 200 °C. Regardless of the operating conditions, a very rapid drop in the alteration rate was observed from the first few days. The rate r_t calculated from the calcium in solution was less than 10^{-6} g m^{-2} d^{-1} (corresponding to the analytical Ca detection limit) (Fig. 4). Two hypotheses can account for the fact that the alteration ceases in this way: the first is based on reaching a thermodynamic equilibrium between the zirconolite and solution, and the second on the formation of an alteration layer with protective properties.

Following a review of published data, thermodynamic calculations were performed to check for saturation of the leachate with respect to the primary phase or secondary phases that likely form and protect the zirconolite surface. Published data on these phases are

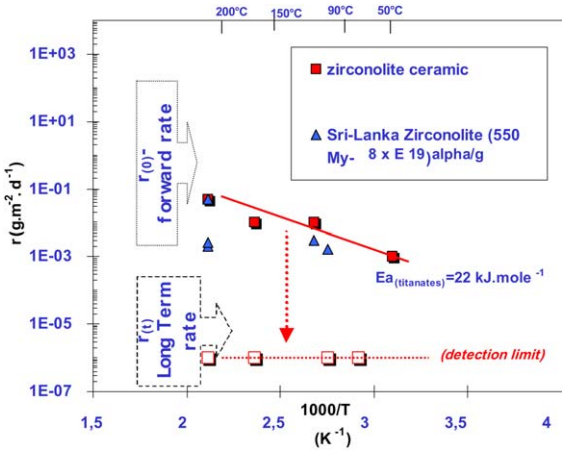

Fig. 4. Leached data for zirconolite ceramics (solid symbols: r_0 initial dissolution rate; empty symbols: r_t long-term rates). The leached data for Sri Lanka natural analogues are from [12].

rare and concern only the pure phases (i.e. without rare-earth elements). Thermodynamic data were therefore obtained by approximation for some phases: Nd-doped zirconolite, $Ti(OH)_4$, oxide mixtures, decalcified zirconolite $Zr_4Ti_8O_{24}$. The approximation method is discussed in detail in reference [9]. The calculated results are indicated in Fig. 5: positive (Q/K) values (activity products of the different chemical species involved in the dissolution reaction/solubility products) correspond to oversaturation of the leachate with respect to the relevant solid phases, and negative values to undersaturation. They show that the cessation of zirconolite alteration in pure water cannot be attributed to a thermodynamic equilibrium between the primary zirconolite phase and solution. Conversely, saturation can be observed with respect to Ti, Zr and Al hydroxides, and oversaturation with respect to a decalcified zirconolite phase. Two schemes could account for the cessation of alteration:

- (*i*) adsorption of water molecules prior to hydrolysis of the Ti–O, Zr–O or Al–O bonds results in the apparent solubility of a hydroxide mixture at the reaction interface; alteration ceases when the hydroxide reaches saturation;
- (*ii*) calcium is leached preferentially, forming a calcium-free zirconolite phase on the surface; alteration continues as long as zirconolite is present at the reaction interface; when the zirconolite is completely decalcified, the alteration ceases.

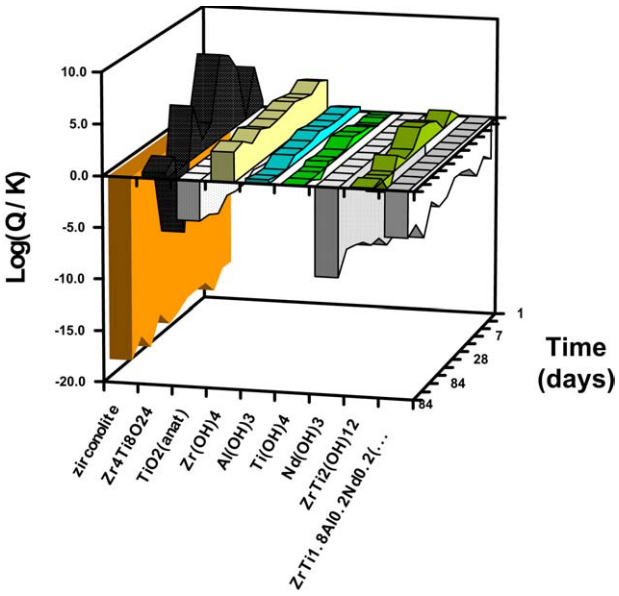

Fig. 5. Saturation index of the leachates with respect to the primary phase (Nd-zirconolite) and some potential secondary phases

Leached surfaces were examined by Scanning Electron Microscopy (SEM), Atomic Force Microscopy (AFM) and Secondary Ion Mass Spectrometry (SIMS) to confirm the hypothesis that a protective layer forms on the zirconolite surface. An alteration layer about 10 nm thick was observed by SEM and AFM (Fig. 6); it was impossible to determine the chemical composition of this layer by SIMS because of its roughness.

Chemical durability studies of the Nd-doped zirconolite ceramic revealed the high quality of the matrix. These results were corroborated by Gieré et al [10], who investigated zirconolite alteration under hydrothermal conditions between 150 and 700 °C in the presence of various types of fluids (deionised water,

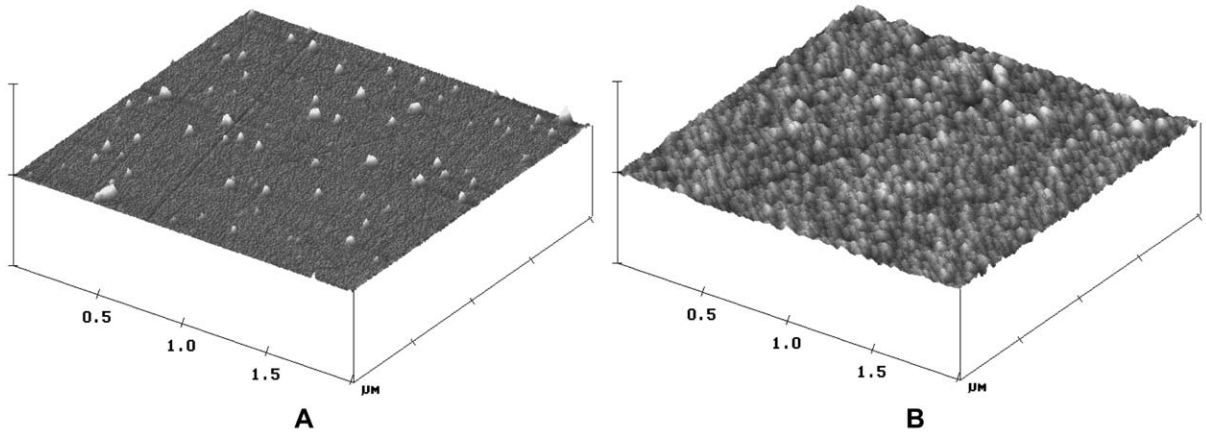

Fig. 6. AFM map of fresh zirconolite (**a**) and altered zirconolite (**b**) (dots on fresh zirconolite are dust particles from polishing).

NaOH, HCl, H_3PO_4, etc.). At temperatures below 250 °C, the matrix alteration was extremely low. The conservation of these properties must now be demonstrated after α self-irradiation.

2.2.2. Matrix behaviour under irradiation

Cylindrical zirconolite ceramic pellets containing 10 wt% Nd_2O_3 were exposed to bombardment on both main faces by lead ions (Pb^{3+}) at two doses 3×10^{14} ions cm^{-2} corresponding to the critical amorphization dose (D_c) and 2×10^{16} ions cm^{-2} in the IRMA facility at the Orsay Nuclear Spectrometry and Mass Spectrometry Centre (France). The crystalline structure was damaged to a depth of about 100 nm and became completely amorphous. The aqueous corrosion resistance was measured in Soxhlet mode at 100 °C in initially pure water [11]. Similar behaviour was observed in the ceramic before and after irradiation (Fig. 7):

- (*i*) alteration under initial rate r_0 conditions was observed for the first 24 to 48 h; for the two doses, the initial alteration rate of the damaged zirconolite was the same as for the crystalline ceramic (within a factor of 1.5), equivalent to an altered thickness of about 10 nm;
- moreover, after the initial transient step lasting a few days, the alteration rate dropped significantly and in the same way for both materials by more than four orders of magnitude (to 10^{-6} g m^{-2} d^{-1}).

Published data concerning natural zirconolite enriched in thorium (20 wt% ThO_2) 550 million years old and completely metamict (after being subjected to between 5×10^{18} and 2.5×10^{21} α disintegrations g^{-1}) are indicated in the Arrhenius diagram (Fig. 4) [12]. The initial alteration rate of these metamict samples is similar to that of perfectly crystallized Nd-doped zirconolite. The data show that, even after sustaining α self-irradiation damage, the chemical durability of the matrix is not fundamentally modified.

Data for synthetic ceramics bombarded with heavy ions and natural metamict zirconolite enriched in thorium show that the chemical durability of the matrix is not significantly affected under initial rate (r_0) conditions. It is, of course, necessary to demonstrate that the containment performance of the matrix is conserved under α self-irradiation. Zirconolite ceramic samples doped with short-lived actinides ($Ca_{0.87}Pu_{0.13}ZrTi_{1.73}Al_{0.26}O_7$ with 10wt% $^{238}PuO_2$) were synthesized for this purpose in the Atalante high-level waste (DHA) facility [13]. Zirconolite is the predominant phase with a minor phase enriched in Zr (non detectable using XRD) (Fig. 8 and Fig. 9); these samples are now being examined to assess the behaviour of this matrix under α self-irradiation.

3. Hollandite

The hollandite group of minerals has the general formula $A_xB_yC_{8-y}O_{16}$. The B and C cations are surrounded by an octahedral configuration of oxygens. Each of these $(B,C)O_{16}$ octahedra shares two edges to form paired chains running parallel with the *c*-axis

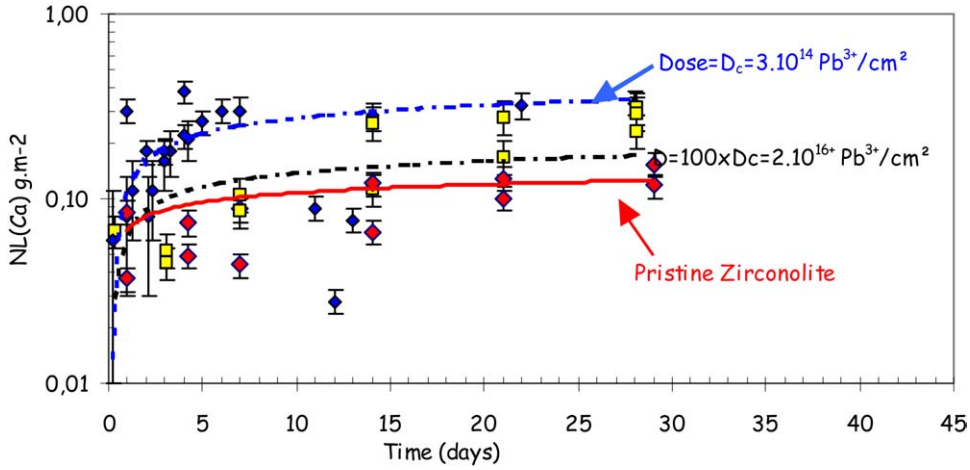

Fig. 7. Soxhlet-mode leaching of Nd-doped zirconolite before and after irradiation by heavy ions. The normalized mass losses in Ca (NL(Ca)) are in red for pristine zirconolite, in blue after irradiation at a dose of 3×10^{14} Pb cm^{-2}, in yellow after irradiation at a dose of 2×10^{16} Pb cm^{-2}.

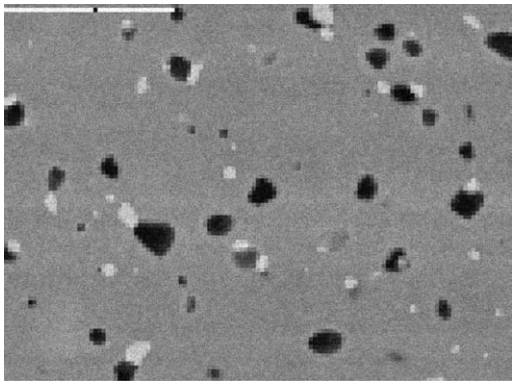

Fig. 8. Backscattered electron image of Pu zirconolite.

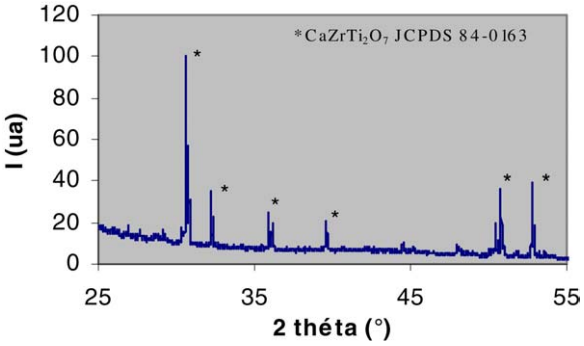

Fig. 9. XRD spectra of zirconolite containing 10wt.% PuO_2.

(Fig. 10). These chains are cross-linked to neighbouring paired-chains to form a 3-dimensional framework with tunnels running parallel to the *c*-axis. The large A cations are located in these tunnels. In Synroc hollandite the A position is occupied by Ba and Cs, the B position by Al and Ti^{3+}, and the C position by Ti^{4+}. The

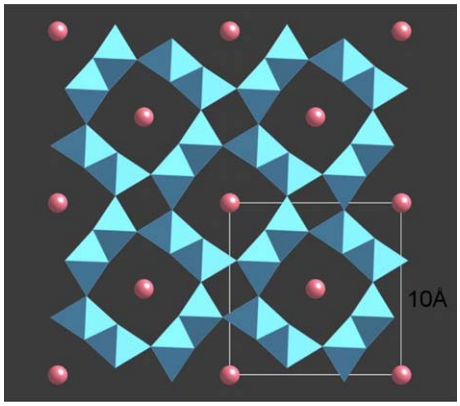

Fig. 10. Crystalline structure of hollandite.

general formula for Synroc titaniferous hollandite is $[Ba_xCs_y][(Ti, Al)^{3+}_{2x+y}]\ Ti^{4+}_{8-2x-y}O_{16}$ [14].

3.1. Synthesis and characterization of hollandite ceramic

The protocol for synthesizing a titaniferous ceramic with the formula $Ba_1Cs_{0.09}(Al_{1.5}Ti_{0.59})^{3+}Ti_{5.91}{}^{4+}\ O_{16}$ (containing 1.5 wt% Cs) was developed by ANSTO.

Kesson et al. [15] showed that three criteria must be met to obtain a hollandite ceramic without minor phases detrimental to the chemical stability of the matrix: (*i*) the trivalent elements (Al^{3+} and Ti^{3+}) must be present in sufficient quantities; (*ii*) the trivalent elements must be not be represented by Al^{3+} alone, but also by Ti^{3+}; (*iii*) the presence of 'reduced rutile' TiO_{2-x} is also indispensable to prevent the formation of secondary phases.

The ceramic is thus synthesized by hydrolysis of an alkoxide mixture of Al and Ti with a nitric acid solution of Ba and Cs, followed by drying the powder, calcining, milling, then adding metallic Ti (about 1.7 wt%) and pressure-assisted sintering under Ar atmosphere. The resulting ceramic is a composite matrix of hollandite (99.5%) and rutile (0.5%).

We therefore undertook the optimisation of the matrix composition in order to simplify the fabrication process. We replaced Ti^{3+} with Fe^{3+} to ensure a sufficient quantity of trivalent elements to avoid the formation of phases with poor chemical durability and to obtain the material by natural sintering in air [16].

The optimised protocol includes the following steps. An amorphous homogeneous powder precursor is first obtained by hydrolysis of a mixture of Al and Ti alkoxides by a nitric acid solution of Ba, Fe and Cs. After hydrolysis, the resulting powder is oven-dried at 120 °C, then calcined for 2 h at 1000 °C and ground. The powder is then pressed at 120 MPa to obtain cylindrical compacts that are sintered in air at 1250 °C for 15 h [17].

The ferriferous hollandite composition range examined was: $Ba_xCs_y(Al,Fe)_{2x+y}Ti_{8-2x-y}O_{16}$, where *x* ranges from 0.5 to 1 and *y* from 0.1 (1.5% Cs_2O) to 0.28 (5%). Hollandite is always the predominant phase (> 99%) with rutile present in some cases. The composition $BaCs_{0.28}(Al_{1.46}Fe_{0.82})Ti_{5.72}O_{16}$ results in a single-phase ceramic containing 4.3 wt% caesium, as observed on the SEM image (Fig. 11) and on the XRD pattern (Fig. 12).

3.2. Chemical durability of hollandite matrices

The initial alteration rates r_0 in initially pure water were determined for titaniferous (1.5% Cs) and ferriferous (4.3% Cs) hollandite ceramics between 50 and 200 °C by assaying caesium (an alteration tracer) in solution. The activation energy E_a of the hydrolysis reaction is about 20 kJ mol^{-1} (Fig. 13) showing slight temperature dependence. At 100 °C, the initial alteration rate of titaniferous hollandite is about 1.2×10^{-2} g m^{-2} d^{-1}; compared with about 4×10^{-2} g m^{-2} d^{-1} for ferriferous hollandite This indicates that partial substitution of iron for titanium does not affect the chemical durability of the matrix. Moreover, as for the zirconolite matrices, the initial dissolution step is transient (a few hours to no more than one day); the rate then diminishes very rapidly – even under conditions with high solution renewal (Soxhlet mode) or in highly dilute solutions. The first step in the alteration process corresponds to an altered thickness of about 10 to 50 nm. This trend must still be confirmed by tests at high *S/V* ratios simulating advanced stages of reaction progress.

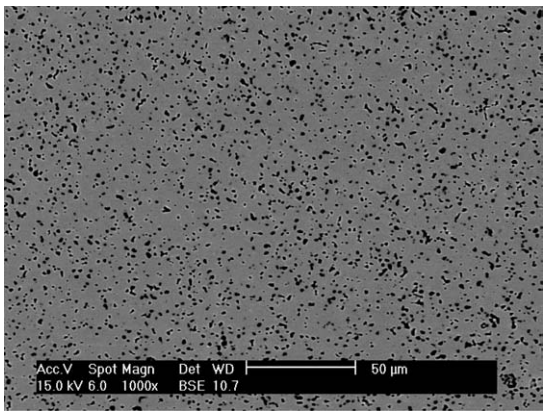

Fig. 11. Backscattered electron image of hollandite $BaCs_{0.28}(Al_{1.46}Fe_{0.82})Ti_{5.72}O_{16}$.

4. Conclusion

Zirconolite and hollandite ceramics have proven to be high-performance matrices for conditioning minor actinides (about 10 wt%) and caesium (about 5 wt%), respectively. Their synthesis protocols have been optimised to obtain a single-phase matrix (with no minor phase of poorer chemical durability) by natural sintering in air. These matrices exhibit high chemical durability with a very low initial alteration rate (about 10^{-2} g m^{-2} d^{-1} at 100°C). Transient initial-rate conditions lasting from a few hours to one day are observed for both materials, after which the alteration rate drops. Alteration virtually ceases in the case of zirconolite. The excellent chemical durability properties of zirconolite are unaffected even after amorphization of the crystalline structure by external irradiation with heavy ions or by self-irradiation of natural zirconolite specimens 550 million years old. This performance must

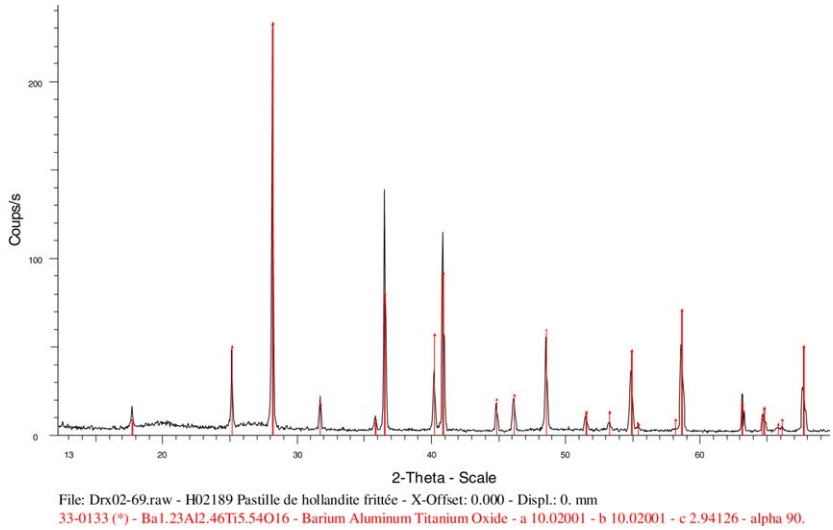

Fig. 12. Diffraction diagram for hollandite $BaCs_{0.28}(Al_{1.46}Fe_{0.82})Ti_{5.72}O_{16}$.

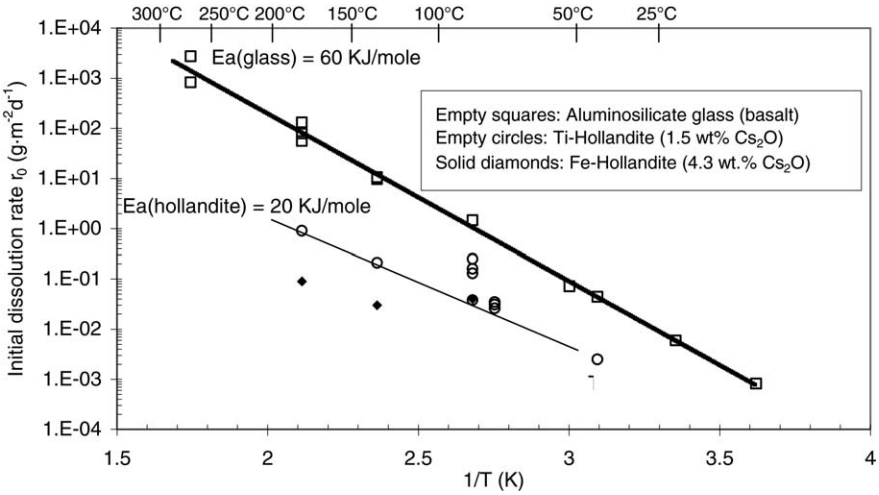

Fig. 13. Leaching data for titaniferous (empty circles) and ferriferous (solid diamonds) hollandite compared with data for aluminosilicate glass (empty squares).

now be confirmed on synthetic matrices doped with short-lived actinides. Zirconolite ceramics containing 10 wt% ^{238}Pu have been fabricated for this purpose in the Atalante high-level waste (DHA) facility. The evolution of the Zirconolite samples and their properties when subjected to α self-irradiation is now a major issue in demonstrating the performance of this type of matrix.

References

[1] A.E. Rngwood, S.E. Kesson, K.D. Reeve, D.M. Levins, E.J. Ramn, in: W. Lutze, R.C. Ewing (Eds.), Radioactive waste forms for the future, 1988, p. 233.
[2] B.D. Begg, E.R. Vance, R.A. Day, M. Hambley, S.D. Conradson, Mater. Res. Soc. Symp. Proc. 465 (1997) 325.
[3] B.D. Begg, R.A. Day, A. Brownscombe, Mater. Res. Soc. Symp. Proc. 663 (2001) 259.
[4] E.R. Vance, P.J. Angel, B.D. Begg, R.A. Day, Mater. Res. Soc. Symp. Proc. 333 (1994) 293.
[5] B.D. Begg, E.R. Vance, B.A. Hunter, J.V. Hanna, J. Mater. Res. 13 (1998) 3181.
[6] G. Leturcq, P.J. McGlinn, K.P. Hart, T. Advocat, C. Barbe, G.R. Lumpkin (to be published).
[7] E.R. Vance, C.J. Ball, M.G. Blackford, D.J. Cassidy, K.L. Smith, J. Nucl. Mater. 175 (1990) 58.
[8] T. Advocat, C. Fillet, F. Bart, G. Leturcq, F. Audubert, J.-E. Lartigue, M. Bertolus, C. Guy, Proceedings of the Global'01, International Conference on Back-End of the Fuel Cycle. 9–13 September, Paris, 2001.
[9] G. Leturcq, T. Advocat, K.P. Hart, G. Berger, J. Lacombe, A. Bonnetier, Am. Mineral. 86 (2001) 871.
[10] R. Gieré, J. Malmström, E. Reusser, G.R. Lumpkin, M. Düggelin, D. Mathys, R. Guggenheim, D. Günther, Mater. Res. Symp. Proc. 663 (2001) 267.
[11] Norme AFNOR expérimentale X 30-403, France, December 1999.
[12] A.E. Ringwood, V.M. Oversby, S.E. Kesson, W. Sinclair, N. Ware, W. Hibberson, A. Major, Nucl. Chem. Waste Manage. 2 (1981) 287–305.
[13] T. Advocat, F. Jorion, T. Marcillat, G. Leturcq, X. Deschanels, J.-M. Boubals, L. Bojat, P. Nivet, S. Peuget, Mater. Res. Symp. Proc., Scientific Basis for Nuclear Waste Management (under press).
[14] S.E. Kesson, Radioact. Waste Manage. Nucl. Fuel Cycle 4 (1983) 53.
[15] (a) S.E. Kesson, T.J. White, Proc. R. Soc. Lond. A 405 (1986) 73 (Part I); (b) S.E. Kesson, T.J. White, Proc. R. Soc. Lond. A 408 (1986) 295 (Part II).
[16] G. Leturcq, F. Bart, A. Comte, Patent No. EN 01/15972, 11 December 2001.
[17] F. Bart, G. Leturcq, H. Rabiller, in Proc. 105th Annual Meeting & Exposition of The American Ceramic Society, Nashville, USA, 27 April–2 May 2003.